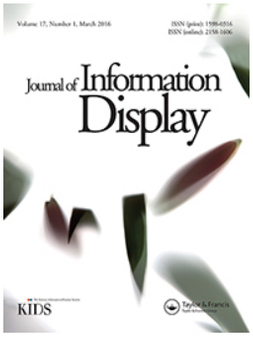

Journal of Information Display

ISSN: 1598-0316 (Print) 2158-1606 (Online) Journal homepage: https://www.tandfonline.com/loi/tjid20

Naphthalene-diimide-incorporated conjugated polyelectrolyte interfacial modifier for the efficient inverted-type polymer solar cells

So Youn Nam, Eun Young Choi, Chang Eun Song, Changjin Lee, In Hwan Jung & Sung Cheol Yoon

To cite this article: So Youn Nam, Eun Young Choi, Chang Eun Song, Changjin Lee, In Hwan Jung & Sung Cheol Yoon (2016) Naphthalene-diimide-incorporated conjugated polyelectrolyte interfacial modifier for the efficient inverted-type polymer solar cells, Journal of Information Display, 17:1, 17-24, DOI: 10.1080/15980316.2016.1139513

To link to this article: https://doi.org/10.1080/15980316.2016.1139513

Published online: 19 Feb 2016.

Journal of Information Display, 2016
Vol. 17, No. 1, 17–24, http://dx.doi.org/10.1080/15980316.2016.1139513

Taylor & Francis
Taylor & Francis Group

Naphthalene-diimide-incorporated conjugated polyelectrolyte interfacial modifier for the efficient inverted-type polymer solar cells

So Youn Nam[a], Eun Young Choi[a,b], Chang Eun Song[a], Changjin Lee[a,b,c], In Hwan Jung[a,c*] and Sung Cheol Yoon[a,b,c*]

[a]*Advanced Materials Division, Korea Research Institute of Chemical Technology (KRICT), Daejeon 305-600, Republic of Korea;* [b]*Department of Nanomaterials Science and Engineering, University of Science and Technology (UST), Daejeon 305-350, Republic of Korea;* [c]*Department of Chemical Convergence Materials, University of Science and Technology (UST), Daejeon 305-350, Republic of Korea*

(*Received 26 November 2015; accepted 29 December 2015*)

A cationic conjugated polyelectrolyte (PFTNDI) containing electron-accepting naphthalene diimide moiety was designed and synthesized to improve the surface properties of the ZnO layer in the inverted polymer solar cells (PSCs). After the PFTNDI treatment of the ZnO surface, the uniformity and hydrophobicity of the surface was significantly enhanced, resulting in highly reduced surface tension. In addition, the permanent interfacial dipole at the interface of ZnO and PFTNDI induced a shift in the vacuum level, leading to the reduced work function (WF) of the ZnO layer. The inverted devices with an ITO/ZnO/PFTNDI/PTB7-Th:$PC_{71}BM$/MoO_3/Ag configuration were fabricated, and the photovoltaic properties were investigated. The reduced WF of the ZnO film resulted in slightly increased V_{oc} values and highly reduced contact resistance. Combined with reduced surface tension, the PFTNDI-treated devices exhibited much higher power conversion efficiency (8.65%) than the bare ZnO devices (7.99%).

Keywords: naphthalene diimide; polyelectrolyte; interfacial modifier; inverted-type polymer solar cells

Introduction

For decades, polymer solar cells (PSCs) have been extensively studied and have shown potential commercial application. Bulk heterojunction-type cells based on a polymer/[6,6]-phenyl-C_{71}-butyric-acid-ester-($PC_{71}BM$)-blended active layer have demonstrated over 10% power conversion efficiencies (PCE) [1–3]. PSCs have unique advantages, such as being lightweight, solution processability, and flexibility, as opposed to inorganic solar cells [4–7], and could be classified as a conventional or an inverted architecture. The inverted device was designed to overcome the drawback of the conventional structure consisting of ITO/poly(3,4-ethylene-dioxythiophene):poly(styrenesulfonate) (PEDOT:PSS)/ active layer/Al. PEDOT:PSS is an excellent hole transport polymer, but its high acidity (pH1-2) causes the chemical degradation of the ITO electrode, which is a serious problem in terms of long-term stability. In addition, low-WF metals such as calcium, barium, and aluminum can be easily oxidized when exposed to oxygen or moisture, resulting in the fast degradation of the PCE [8,9]. In the inverted structure, the low WF metals have been replaced by ITO doped with transparent oxides such as zinc oxide or titanium dioxide. As an anode, air-stable high-WF metals such as Ag and Au, which could be easily printed in open air, have been applied. Thus, the inverted device commonly shows the following configurations: ITO/ZnO/active layer/MoO_3/Ag. Air-stable ZnO has been regarded as a promising candidate for the electron-transporting and hole-blocking layer because of its high electron mobility, transmittance, and solution processability [10–12]. The surface properties of ZnO films, however, are not ideal in the inverted structure: the terminal hydroxyl groups of the ZnO film surface are working as electron-trapping sites, and the hydrophilic surface makes poor contact with the hydrophobic active layer [13,14]. To improve the surface properties of the ZnO film, several polyelectrolytes (PEs) with polar side chains [15–17] have been developed and introduced on the ZnO surface. The design concept is that the hydrophilic side chain is bonded to the ZnO surface through electrostatic interaction, and the hydrophobic polymer backbone is exposed towards the active layer to reduce the surface tension of the ZnO surface. In addition, the dipole moment generated at the interface of ZnO/PE has an effect on the WF of the cathode, promoting the electron transfer process [18].

In this study, a new conjugated PE, poly[(9,9-bis(6′-N,N,N-trimethylammoniumhexyl)-9H-fluorene-2,7-diyl)-alt-(2,7-bis(2-hexyldecyl)benzo[lmn][3,8] phenanthroline-1,3,6,8(2H,7H)-tetraone-4,9-diyl)] bromide (PFTNDI),

*Corresponding authors. Email: ihjung@krict.re.kr; yoonsch@krict.re.kr

ISSN (print): 1598-0316; ISSN (online): 2158-1606

containing hydrophilic fluorene (FL) salt and electron-accepting naphthalene diimide (NDI) moiety, was synthesized. The combination of the FL and NDI moieties has also been studied of late for the non-fullerene acceptors in PSCs [19–21]. The NDI moiety in PFTNDI was introduced to improve the hydrophobicity of the ZnO surface and to enhance the electron-transporting properties at the interface of the active layer and ZnO, and the trimethylammonium bromide salt in PFTNDI was to interact with the hydrophilic ZnO surface and to generate the permeant dipole moment at the interface of ZnO/PFTNDI. After the introduction of the PFTNDI layer on the ZnO surface, the surface properties of the ZnO film were dramatically improved. The rough ZnO surface was modified into a highly uniform film, and the hydrophilic ZnO surface was changed to a highly hydrophobic surface. In addition, the PFTNDI was also shifting the vacuum level at the surface of the ZnO film via net dipole formation, resulting in the enhancement of the open-circuit voltage (V_{oc}) in the devices. The NDI-incorporated PE was successfully working as an interfacial modifier (IM), and the 7.99% PCE of the inverted devices was enhanced into 8.65% after the PFTNDI treatment of the ZnO surface. The IM effects will be discussed in detail in terms of the surface morphology, molecular energy levels, and photovoltaic J–V characteristics.

Results and discussion

Synthesis and characterization

4,9-dibromo-2,7-bis(2-hexyldecyl)benzo[lmn][3,8]phenanthroline-1,3,6,8(2*H*,7*H*)-tetraone (NDI-br) [22] and 2,2′-(9,9-bis(6-bromohexyl)-9*H*-fluorene-2,7-diyl)bis(4,4,5,5-tetramethyl-1,3,2-dioxaborolane) (F-B) [23] were synthesized according to the literature procedure. The PFTNDI PE was obtained via a two-step process of polymerization and quaternization. The precursor polymer, PFNDI, was synthesized through the Suzuki coupling of NDI-br and F-B. It showed excellent solubility in common organic solvents (e.g. THF, toluene, and dichloromethane) and a sizable average molecular weight (M_n) of 31,000 (PDI = 2.43) determined via gel permeation chromatography (GPC), using polystyrene as a standard. The alcohol-soluble conjugated PE, PFTNDI, was obtained through PFNDI treatment with trimethylamine in a mixture of THF and methanol for two days. The final PFTNDI polymer is soluble only in highly polar solvents (e.g. methanol, DMSO, and DMF) due to the ionic charge formation of quaternary ammonium salt. The degree of quaternization was estimated to be > 95% from the integration of the ^{1}H NMR spectra and from the comparison of the peaks at 3.07 ppm ($-N+(CH_3)_3Br-$) and at 8.73 ppm (aromatic proton at NDI monomer). The ^{1}H NMR spectra of PFNDI and PFTNDI are shown in 'Supporting Information'. The synthetic routes to the PFNDI and PFTNDI are outlined in Scheme 1.

The absorption spectra of PFNDI and PFTNDI were recorded in solution and in films. The spectra are shown in Figure 1(a) and are summarized in Table 1. In the solution, the two polymers showed almost identical absorption spectra even with different solvent systems: chloroform for PFNDI and DMF for PFTNDI. In the film, PFNDI showed 14 nm more red-shifted absorption maximum than in the solution, but PFTNDI showed an absorption spectrum almost similar to that in the solution. It is expected that PFNDI will make better π-π molecular stacking in the film state, but PFTNDI interrupts the molecular ordering in the film states due to the hydrophilic–phobic repulsion caused by the ionic-charge groups. The optical bandgaps (E_g^{opt}) of PFNDI and PFTNDI were determined from their absorption edges to be 2.05 and 2.12 eV, respectively.

The highest occupied molecular orbital (HOMO) energy level (E_{HOMO}) of PFNDI was determined from cyclic voltammetry (CV) measurement using the oxidation onset potential relative to ferrocene as an internal standard, and the cyclic voltammograms are shown in Figure 1(b). The onset oxidation potential (E_{ox}) of PFNDI was 1.02 V, corresponding to the HOMO energy level of −5.73 eV. The lowest unoccupied molecular orbital (LUMO) energy level (E_{LUMO}) of PFNDI was estimated from the optical

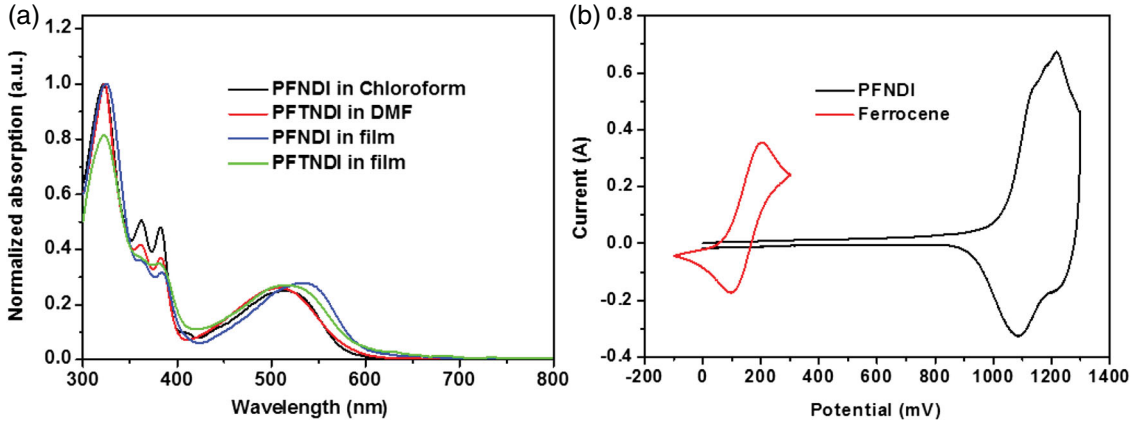

Figure 1. (a) Absorption spectra of PFNDI and PFTNDI in the solution and the film and (b) cyclic voltammogram of PFNDI.

Table 1. Optical and electrochemical properties of PFNDI and PFTNDI.

Polymer	Solution λ_{max} (nm)	Film λ_{max} (nm)[b]	Film $E_{g,opt}$ (eV)[c]	P-doping $E_{ox/onset}$ (V vs. Ag/Ag^+)	P-doping $E_{HOMO,elec}$[d] (eV)	E_{LUMO}[a] (eV)
PFNDI	322, 520[e]	326, 534	2.05	1.02	− 5.73	− 3.68
PFTNDI	323, 520[f]	326, 520	2.12	–	–	–

[a]LUMO energy estimated by adding the absorption onset to the HOMO energy.
[b]Thin film on a quartz plate formed by spin-coating for 60 s at 1500 rpm.
[c]Bandgap calculated from the film-state absorption onset wavelength.
[d]HOMO energy level determined from the E_{onset} of the first oxidation potential of ferrocene, − 4.8 eV.
[e]Dilute solution in chloroform.
[f]In DMF.

Table 2. Surface properties of the PFTNDI-treated and bare ZnO films.

	Contact properties				AFM properties		
	DI[a] (°)	Polar (mN m^{-1})	Disp. (mN m^{-1})	Surface tension (mN m^{-1})	RMS[b] (nm)	Ra (nm)	Rmax (nm)
ZnO	26.7	36.6	30.1	66.8	6.59	5.17	54.8
ZnO + PFTNDI	75.9	5.37	37.7	43.0	1.23	0.792	24.3

[a]Water contact angle.
[b]RMS roughness of the surface.

bandgap and the HOMO energy level, and was calculated as − 3.68 eV. CV results are summarized in Table 1.

Tuning of morphology and WF

The major roles of IM on the ZnO film are surface modification and WF tuning. First, the water contact angle and atomic force microscopy (AFM) images at the surfaces of the ZnO films with or without PFTNDI treatment were measured to determine the differences in the surface properties. After the PFTNDI treatment of the ZnO film, the hydrophobicity of the ZnO surface was significantly enhanced, as shown in Figure 2(b). The PFTNDI-treated film showed a highly enhanced water contact angle (75.9°) and significantly reduced surface tension (43.0 mN m^{-1}) compared to the bare ZnO film. In addition, the rough

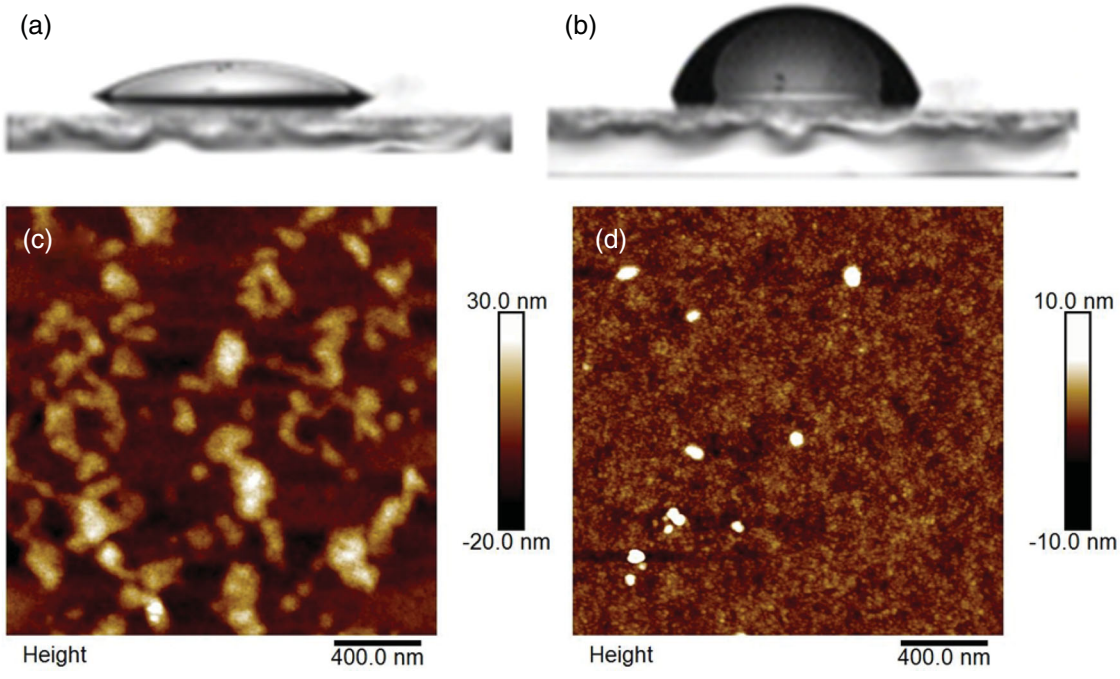

Figure 2. Surface properties of the ZnO film without (a, c) and with PFTNDI treatment (b, d); water contact test of the (a) bare ZnO and (b) PFTNDI-treated ZnO; AFM images of the (c) bare ZnO and (d) PFTNDI-coated ZnO.

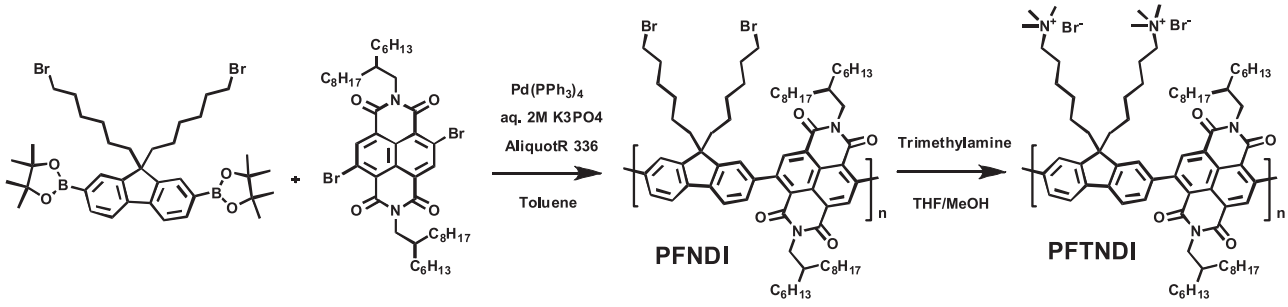

Scheme 1. Synthetic routes for the precursor PFNDI polymer and the final PFTNDI PE.

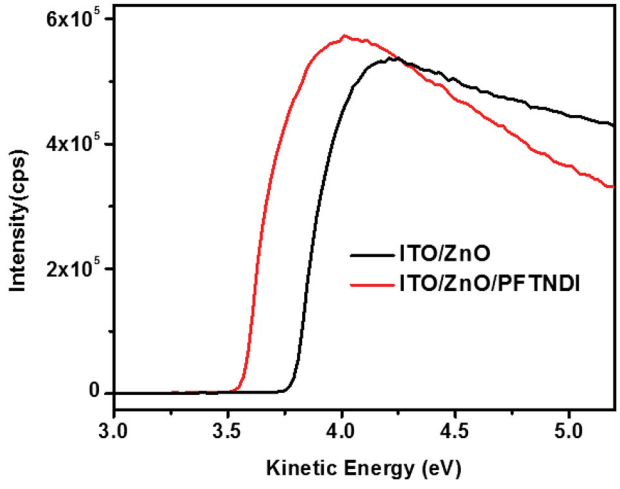

Figure 3. UPS spectra of the ZnO layer with or without PFTNDI in the low-kinetic-energy cut-off.

ZnO surface was changed to a highly uniform surface after PFTNDI treatment. As shown in Figure 2(c) and 2(d), the 6.59 nm root-mean-square (RMS) roughness of the bare ZnO film was highly reduced, approaching that of the ZnO/PFTNDI film (1.23 nm). Surface properties including contact angle and film roughness are summarized in Table 2 and Figure 2.

The enhanced hydrophobicity and uniformity of the ZnO surfaces after PFTNDI treatment give a great advantage in enhancing the contact quality with the hydrophobic active layer. Second, ultraviolet photoelectron spectroscopy (UPS) was carried out to study the differences in WF of the bare ZnO and the ZnO/PFTNDI films. The low-kinetic-energy cut-off (E_{cutoff}) of ZnO and ZnO/PFTNDI were defined as the lowest kinetic energy of the measured electrons, which can be used to estimate the WF, and shown in Figure 3. The WFs of the ITO/ZnO and ITO/ZnO/PFTNDI films were determined to be 3.77 and 3.55 eV, respectively. After PFTNDI treatment, the WF of the ZnO layer was successfully shifted by 0.22 eV towards the vacuum level, indicating that the net dipoles at the interfaces were pointing towards the active layer [18]. The modified WF has an effect on the open-circuit voltage (V_{oc}) of photovoltaic devices. The maximum V_{oc} is determined by the energy difference between the quasi-Fermi levels of the photo-induced holes in the donor (PTB7-Th) and the photo-induced electrons in the acceptor ($PC_{71}BM$) under illumination, but the maximum V_{oc} is reduced by the static internal electric field across the device, which is a result of the difference between the WFs of the electrodes [24]. Therefore, the reduced WF after PFTNDI treatment could have a positive effect on the V_{oc} characteristic in photovoltaic devices.

Photovoltaic properties

To improve the photovoltaic properties of ZnO-based BHJ photovoltaic devices, the PFTNDI solution (0.05 wt%) in DMF was spin-coated on the ZnO film, and the devices were fabricated with the following configuration: ITO/ZnO/PFTNDI/PTB7-Th:$PC_{71}BM$/MoO_3/Ag. The J–V characteristics of the devices measured under an AM 1.5G solar simulator with a power density of 100 W/cm^2 are shown in Figure 4(a), and the corresponding photovoltaic parameters are summarized in Table 3. The typical inverted devices without IM treatment showed a PCE of 7.99% with a V_{oc} of 0.797 V, a J_{sc} of 16.41 mA cm^{-2}, and an fill factor (FF) of 61%. After PFTNDI treatment, the photovoltaic performance was enhanced as a PCE of 8.65% with a V_{oc} of 0.809 V, a J_{sc} of 16.47 mA cm^{-2}, and an FF of 65%. The J_{sc} values of both devices were almost identical, which was confirmed by the external quantum efficiency (EQE) shown in Figure 4(c). The V_{oc} was slightly enhanced by as much as 0.012 V. This originated from the reduced WF of ZnO due to the permanent interfacial dipole formed between the positive quaternary amine and the negative bromide ion. Much of the improvement in the device performance was caused by the FF, which is closely related to the series (R_s) and shunt (R_{sh}) resistance. The PFTNDI-treated devices showed a highly reduced R_s value of 1.28 Ω cm^2 and a one-order-higher R_{sh} (around 10^4 Ω cm^2) than the devices without PFTNDI treatment. It is well known that the R_s value results from the resistance of the contacts between the active layer and the electrode, and the R_{sh} values, from the leakage current providing an alternate current path for the light-generated current _ENREF_39 [25]. As shown in Figure 4(b), the series resistance and leakage current in the dark were significantly reduced after PFTNDI treatment.

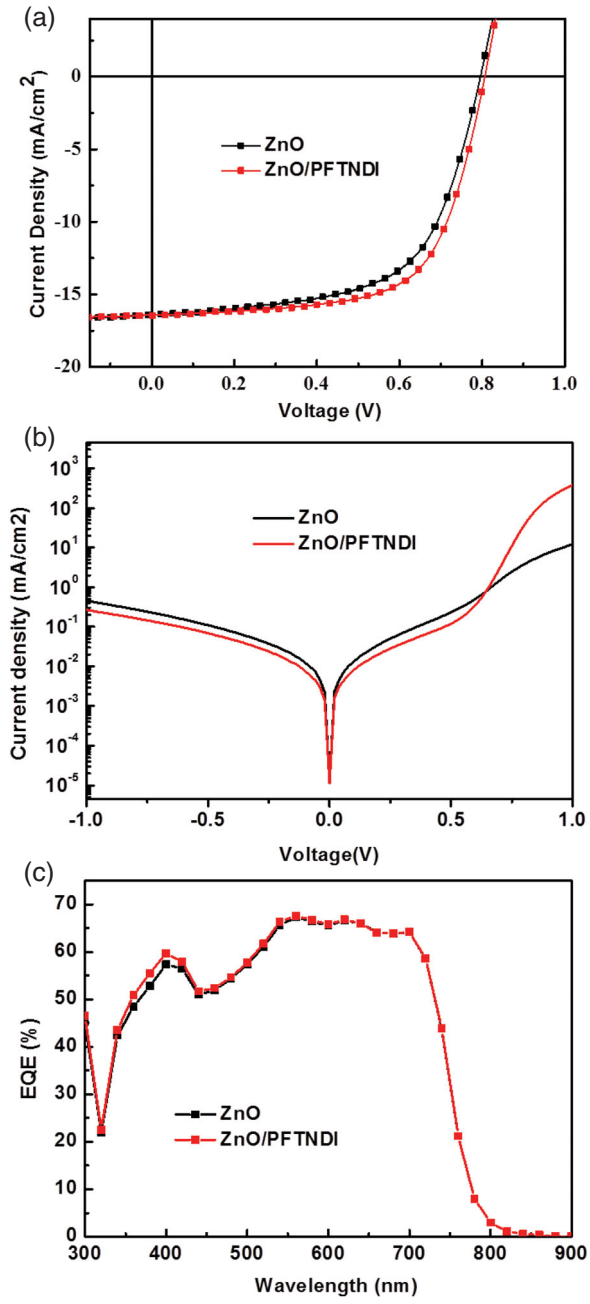

Figure 4. Current density (J) vs. voltage (V) characteristics of the ZnO and ZnO/PFTNDI devices measured (a) under AM 1.5G simulated light illuminations with 100 mW/cm^2 intensity in air, (b) in the dark, and (c) EQE of the BHJ photovoltaic devices with an active layer composed of PTB7-Th:$PC_{71}BM$ devices with or without PFTNDI treatment.

As a result, the better contact properties at the interfaces after the introduction of PFTNDI successfully enhanced the photovoltaic performance. It is believed that the enhanced contact properties were mainly caused by the reduced surface tension of the ZnO film and the decreased WF of ZnO. First, the enhanced uniformity and hydrophobicity of the ZnO surface after PFTNDI treatment highly reduced the surface tension at the interface with the active layer, improving the contact properties. Second, the reduced WF of the ZnO surface could reduce the contact resistance by promoting ohmic contact at the interface of ITO/ZnO/PFTNDI.

Conclusion

A new conjugated PE, cationic conjugated PE (PFTNDI), was synthesized and applied to the top of the ZnO surface to enhance the interfacial contact with the active layer and to tune the WF of the ITO/ZnO electrode. The interfacial dipole moment at the interface of ZnO/PFTNDI effectively reduced the WF of the ITO/ZnO electrode, resulting in highly decreased series resistance in the photovoltaic devices. In addition, PFTNDI treatment significantly enhanced the uniformity and hydrophobicity of the ZnO surface, resulting in better contact with hydrophobic active layer. As a result, the PTB7-Th/$PC_{71}BM$ device treated with PFTNDI exhibited a highly improved (8.65%) PCE compared to the typical inverted devices (7.99%).

Experiment section

Suzuki polymerization for PFNDI

To a 4,9-dibromo-2,7-bis(2-hexyldecyl)benzo[lmn][3,8] phenanthroline-1,3,6,8(2*H*,7*H*)-tetraone (0.1762 g, 0.202 mmol) and 2,2′-(9,9-bis(6-bromohexyl)-9*H*-fluorene-2,7-diyl)bis(4,4,5,5-tetramethyl-1,3,2-dioxaborolane) (0.1503 g, 0.202 mmol) mixture, 10 mg $(PPh_3)_4Pd(0)$ was added as a catalyst in a dry box. Subsequently, a 2M aqueous K_3PO_4 solution (4.0 mL) was degassed for 30 min, and the phase transfer catalyst Aliquat® 336 in toluene (10 ml) was also purged with nitrogen for 20 min. Both the degassed solutions were transferred to the above mixture via a cannula. After the heating of the mixture under reflux for 24 h, the reaction mixture was cooled to room temperature and was precipitated into methanol (150 mL) through viscous stirring. The polymer fibers were collected via filtration and were sequentially purified through Soxhlet extraction in methanol, acetone, and chloroform. Neutral precursor polymers were finally obtained after drying *in vacuo* at 40°C. [Reddish purple fiber (180 mg, 75%). ^{1}H NMR (400 MHz, $CDCl_3$): 8.81 (s, 2H), 7.94 (d, 2H), 7.51 (m, 4H), 4.07 (br, 4H), 3.32 (t, 4H), 2.00 (br, 4H), 1.73 (br, 2H), 1,25 (br, 68H), 0.85 (16H). Anal. Calcd for $C_{71}H_{98}Br_2N_2O_4$: C, 70.87; H, 8.21; N, 2.33, Found: C, 69.8; H, 8.5; N, 2.3].

Quaternization for PFTNDI

Condensed trimethylamine (3–5 mL) was added dropwise to a solution of the neutral precursor PFNDI polymer (100 mg) in tetrahydrofuran (10 mL) at −78°C. The mixture was allowed to warm up to room temperature overnight. The precipitate was re-dissolved through the addition of excess methanol, and 2 mL trimethylamine was added at −78°C. The resulting mixture was further stirred

Table 3. Device performance parameters of the PTB7-Th:$PC_{71}BM$ solar cells.

Condition	V_{oc} (V)	J_{sc} (mA cm^{-2})	FF (%)	PCE[a] (%)	R_{sh}[b] ($\Omega \cdot cm^2$)	R_s[c] (Ω cm^2)
ZnO only	0.797 ± 0.005	16.41 ± 0.251	0.61 ± 0.004	7.99 ± 0.105	8.6×10^3	7.83
ZnO + PFTNDI	0.809 ± 0.006	16.47 ± 0.146	0.65 ± 0.004	8.65 ± 0.043	1.3×10^4	1.29

[a]Average values in the four devices with the following configuration: ITO/ZnO/PFTNDI or not/PTB7-Th:$PC_{71}BM/MoO_3$/Ag.
[b]Shunt resistance (R_{sh}).
[c]Series resistance (R_s) deduced from the I–V curve in the dark.

for 24 h at room temperature. After the removal of the solvents and of the excess trimethylamine under reduced pressure, diethyl ether was added to precipitate the conjugated PE. The precipitated polymer was collected via filtration and was dried under vacuum. Reddish purple salts, PFTNDI, were obtained. [(90 mg, 82%) ^{1}H NMR (400 MHz, CD_3OD): 8.73 (s, 2H), 8.07 (br, 2H), 7.65 (br, 4H), 4.15 (br, 4H), 3.29 (t, 4H), 3.07 (s, 18H), 2.05 (br, 4H), 1.67 (br, 2H), 1,42 (br, 68H), 0.87 (16H). Anal. Calcd for $C_{77}H_{116}Br_2N_4O_4$: C, 69.98; H, 8.85; N, 4.23, Found: C, 67.2; H, 8.4; N, 3.9].

Measurements

The ^{1}H NMR spectra were recorded on a Bruker Ascend^{TM}-400 spectrometer, with tetramethylsilane as an internal reference. The absorption spectra were measured on a SHIMADZU/UV-2550 model UV-visible spectrophotometer. CV was performed on a BAS 100B/W electrochemical analyzer with a three-electrode cell in a 0.1 N Bu_4NBF_4 solution in acetonitrile at a scan rate of 50 mVs^{-1}. A Pt wire electrode was coated with a film of each polymer by dipping the electrode into a polymer solution in chloroform. All the measurements were calibrated against an internal standard of ferrocene (Fc), whose ionization potential (IP) value is -4.8 eV for the Fc/Fc + redox system. AFM was performed using the tapping mode, and AFM scan images (2×2 μm) were achieved in the tapping mode on Nanoscope from Bruker. The contact angle and surface tension values were measured with Phoenix 300 from SEO Co., Ltd., using DI and diiodomethane.

Ultraviolet photoelectron spectroscopy (UPS)

A set of samples were analyzed using the AXIS Ultra DLD model (KRATOS Inc.) in Korea Basic Science Institute (KBSI), Daejeon. The He I (21.2 eV) emission line was employed as a UV source. The helium pressure in the analysis chamber during the analysis was about 4.0×10^{-8} Torr. The WFs were determined using the incident photon energy, hv = 21.2 eV, E_{cutoff}, and E_{onset}.

Fabrication of photovoltaic devices

The photovoltaic devices were fabricated with the ITO/ZnO/PFTNDI/PTB7-Th:$PC_{71}BM/MoO_3$/Ag structure. The ITO surface was cleaned via sonication and rinsing in distilled H_2O, acetone, and isopropanol. An electron-transporting ZnO layer (30 nm) was spin-coated onto each ITO substrate, and then the PFTNDI (0.05 wt%) in the DMF was spin-coated at 4000 rpm for 30 sec on the ZnO layer. The polymer solution for the active layer was prepared by dissolving the polymer (12 mg mL^{-1}) with $PC_{71}BM$ in chlorobenzene:DIO (97:3 v/v%). The PTB7-Th:$PC_{71}BM$ blended solutions were spin-coated onto the IM-treated ZnO layer. MoO_3 and Ag were deposited sequentially under $< 3 \times 10^{-6}$ Torr vacuum pressure, resulting in a 0.09 cm^2 active area. The thickness of the active layer was measured using a KLA Tencor Alpha-Step IQ surface profilometer. The current density–voltage (J–V) characteristics of the photovoltaic cells were determined by illuminating the cells with simulated solar light (AM 1.5G) at 100 mW cm^{-2} intensity, using a Yamashita Denso 1000 W solar simulator. The electronic data were recorded using a Keithley 236 source-measure unit. The measurements were carried out after masking all but the active cell area of the fabricated device. All the characterizations were carried out under ambient conditions. The illumination intensity was calibrated using a standard Si photodiode detector acquired from PV Measurements Inc., which was calibrated at the National Renewable Energy Laboratory (NREL). The EQE was measured as a function of the wavelength under ambient conditions, in the range of 300–900 nm, using a xenon short arc lamp as the light source (McScience K3100 EQX). Calibration was performed using a-Si reference photodiode.

Funding

This work was supported by a grant from the New & Renewable Energy Core Technology Program of the Korea Institute of Energy Technology Evaluation and Planning (KETEP) funded by the Ministry of Trade, Industry, & Energy of the Republic of Korea [20143010011890].

Notes on contributors

So Youn Nam received her B.S. in Chemical and Biological Engineering degree from Hanbat National University in 2002. Since 2005, she has been a researcher in Korea Research Institute of Chemical Technology (KRICT).

Eun Young Choi received her B.S. in Chemical Engineering degree in 2014 from Chungnam National University. Since 2014, she has been taking a master's course on nanomaterials science and engineering in the University of Science and Technology (UST), under the direction of Dr. Sung Cheol Yoon.

Chang Eun Song received his M.S. and Ph.D. in Materials Science and Engineering degrees from Korea Advanced Institute of Science and Technology (KAIST), Republic of Korea in 2011 and 2014, respectively. Since 2014, he has been a senior researcher in Korea Research Institute of Chemical Technology (KRICT). His current research interest is the device engineering of the solution-processed organic solar cells and perovskite solar cells.

Changjin Lee received his Ph.D. in Chemistry degree in 1989 from the University of Minnesota, USA, and was a postdoctoral researcher at the University of Texas, Austin for two years. He joined Korea Research Institute of Chemical Technology (KRICT) in 1991 and served as the director of the Device Materials Research Center from 2008 to 2011, and as the director of the Advanced Materials Division from 2011 to 2013. He also served as the chairman of the Molecular Electronics Division of the Korea Polymer Society in 2010. He has been a member of the board of directors of Korea Printed Electronics Association since 2010, and a chief major professor in the Department of Chemical Convergence Materials of the University of Science and Technology since 2014. He is currently the chairman of the Macromolecular Chemistry Division of Korean Chemical Society. His main research interest is the development of organic electronic materials and photocuring materials.

In Hwan Jung received his Ph.D. in Chemistry degree in 2011 from Korea Advanced Institute of Science and Technology (KAIST), Republic of Korea, under the direction of Professor Hong-Ku Shim. He then moved to the University of Chicago in the U.S. as a postdoctoral researcher, and studied under Prof. Luping Yu for three years (2011–2014). Since 2014, he has been a senior researcher in Korea Research Institute of Chemical Technology (KRICT), and he is currently an assistant professor in the University of Science and Technology (UST). His current research interest is the development of new organic conjugated materials for photovoltaic application.

Dr. Sung Cheol Yoon received his Ph.D. degree in 1997 from Seoul National University (SNU), Republic of Korea, under the direction of Professor Kyongtae Kim. After graduation, he joined Samsung Total R&D Center in Daejeon, Republic of Korea to develop a single-site catalyst for polyolefin as a senior researcher, a position that he held for four years (1997–2001). Then he moved again to LG Electronics Institute of Technology in Seoul, Republic of Korea to develop phosphorescent OLED materials as a principal researcher, a position that he held for three years (2001–2004). He was also a visiting scholar at the University of Illinois in Chicago (UIC) in the U.S. for one year (2015–2016). Since 2004, he has been a principal researcher in Korea Research Institute of Chemical Technology (KRICT), and since 2012, a professor in the University of Science and Technology (UST). He is interested in the semiconducting materials for organic and printed electronics.

References

[1] Y. Liu, J. Zhao, Z. Li, C. Mu, W. Ma, H. Hu, K. Jiang, H. Lin, H. Ade, and H. Yan, *Nat. Commun.* **5**, 5293 (2014).

[2] C. Liu, C. Yi, K. Wang, Y. Yang, R.S. Bhatta, M. Tsige, S. Xiao, and X. Gong, *ACS Appl. Mater. Interfaces.* **7**, 4928 (2015).

[3] V. Vohra, K. Kawashima, T. Kakara, T. Koganezawa, I. Osaka, K. Takimiya, and H. Murata, *Nat. Photon.* **9**, 403 (2015).

[4] C.J. Brabec, N.S. Sariciftci, and J.C. Hummelen, *Adv. Funct. Mater.* **11**, 15 (2001).

[5] S. Günes, H. Neugebauer, and N.S. Sariciftci, *Chem. Rev.* **107**, 1324 (2007).

[6] M. Helgesen, R. Sondergaard, and F.C. Krebs, *J. Mater. Chem.* **20**, 36 (2010).

[7] B. Zhao, Z. He, X. Cheng, D. Qin, M. Yun, M. Wang, X. Huang, J. Wu, H. Wu, and Y. Cao, *J. Mater. Chem.* **C2**, 5077 (2014).

[8] M. Jørgensen, K. Norrman, and F.C. Krebs, *Sol. Energy Mater. Sol. Cells.* **92**, 686 (2008).

[9] E. Voroshazi, B. Verreet, A. Buri, R. Müller, D. Di Nuzzo, and P. Heremans, *Org. Electronics.* **12**, 736 (2011).

[10] K. Zilberberg, J. Meyer, and T. Riedl, *J. Mater. Chem.* **C1**, 4796 (2013).

[11] S. Kim, C.-H. Kim, S.K. Lee, J.-H. Jeong, J. Lee, S.-H. Jin, W.S. Shin, C.E. Song, J.-H. Choi, and J.-R. Jeong, *Chem. Comm.* **49**, 6033 (2013).

[12] Z. Yin, Q. Zheng, S.-C. Chen, D. Cai, L. Zhou, and J. Zhang, *Adv. Energy Mater.* **4**, 1301404 (2014).

[13] R. Lampande, G.W. Kim, R. Pode, and J.H. Kwon, *RSC Adv.* **4**, 49855 (2014).

[14] S.H. Eom, M.-J. Baek, H. Park, L. Yan, S. Liu, W. You, and S.-H. Lee, *ACS Appl. Mater. Interfaces.* **6**, 803 (2014).

[15] Y.-M. Chang and C.-Y. Leu, *J. Mater. Chem. A.* **1**, 6446 (2013).

[16] T. Yang, M. Wang, C. Duan, X. Hu, L. Huang, J. Peng, F. Huang, and X. Gong, *Energy Environ. Sci.* **5**, 8208 (2012).

[17] A.K.K. Kyaw, D.H. Wang, V. Gupta, J. Zhang, S. Chand, G.C. Bazan, and A.J. Heeger, *Adv. Mater.* **25**, 2397 (2013).
[18] B.H. Lee, I.H. Jung, H.Y. Woo, H.-K. Shim, G. Kim, and K. Lee, *Adv. Funct. Mater.* **24**, 1100 (2014).
[19] H. Patil, A. Gupta, B. Alford, D. Ma, S.H. Privér, A. Bilic, P. Sonar, and S.V. Bhosale, *Asian. J. Org. Chem.* **4**, 1096 (2015).
[20] A. Gupta, X. Wang, D. Srivani, B. Alford, V. Chellappan, A. Bilic, H. Patil, L.A. Jones, S.V. Bhosale, P. Sonar, and S.V. Bhosale, *Asian J. Org. Chem.* **4**, 800 (2015).
[21] A. Gupta, R.V. Hangarge, X. Wang, B. Alford, V. Chellapan, L.A. Jones, A. Rananaware, A. Bilic, P. Sonar, and S.V. Bhosale, *Dyes Pigment.* **120**, 314 (2015).
[22] Y. Kim, J. Hong, J.H. Oh, and C. Yang, *Chem. Mater.* **25**, 3251 (2013).
[23] K.-Y. Pu, Z. Fang, and B. Liu, *Adv. Funct. Mater.* **18**, 1321 (2008).
[24] C.-C. Chueh, C.-Z. Li, and A.K.Y. Jen, *Energy Environ. Sci.* **8**, 1160 (2015).
[25] H.I. Kim, T.T.T. Bui, G.-W. Kim, G. Kang, W.S. Shin, and T. Park, *ACS Appl. Mater. Interfaces.* **6**, 15875 (2014).